AD-A048 327 CASE WESTERN RESERVE UNIV CLEVELAND OHIO DEPT OF ELE--ETC F/G 20/5
PARAMETER STUDIES RELATIVE TO AN ELECTRIC FIELD-INDUCED DIPOLE --ETC(U)
NOV 77 P C CLASPY DAAG29-76-G-0189

UNCLASSIFIED ARO-13807.1-PX NL

| OF |
AD
A048 327

END
DATE FILMED
2-78
DDC

PARAMETER STUDIES RELATIVE TO AN ELECTRIC FIELD-INDUCED DIPOLE MOMENT LASER

FINAL REPORT

PAUL C. CLASPY

17 NOVEMBER 1977

U.S. ARMY RESEARCH OFFICE

GRANT NO. DAAG 29 76G 0189

DEPARTMENT OF ELECTRICAL ENGINEERING AND APPLIED PHYSICS

CASE WESTERN RESERVE UNIVERSITY
CLEVELAND, OHIO 44106

THE FINDINGS IN THIS REPORT ARE NOT TO BE CONSTRUED AS AN OFFICIAL DEPARTMENT OF THE ARMY POSITION, UNLESS SO DESIGNATED BY OTHER AUTHORIZED DOCUMENTS.

Unclassified

SECURITY CLASSIFICATION OF THIS PAGE (When Data Entered)

REPORT DOCUMENTATION PAGE

READ INSTRUCTIONS BEFORE COMPLETING FORM

1. REPORT NUMBER

2. GOVT ACCESSION NO.

3. RECIPIENT'S CATALOG NUMBER

4. TITLE (and Subtitle)
Parameter Studies Relative to an Electric Field-Induced Dipole Moment Laser.

5. TYPE OF REPORT & PERIOD COVERED
Final Report.
1 April 1976-31 July 1977

6. PERFORMING ORG. REPORT NUMBER

7. AUTHOR(s)
Paul C. Claspy

8. CONTRACT OR GRANT NUMBER(s)
DAAG 29 76G 0189

9. PERFORMING ORGANIZATION NAME AND ADDRESS
Electrical Engineering & Applied Physics
Case Western Reserve University
Cleveland, Ohio 44106

10. PROGRAM ELEMENT, PROJECT, TASK AREA & WORK UNIT NUMBERS

11. CONTROLLING OFFICE NAME AND ADDRESS
U. S. Army Research Office
Post Office Box 12211
Research Triangle Park, NC 27709

12. REPORT DATE
17 November 1977

13. NUMBER OF PAGES
34

14. MONITORING AGENCY NAME & ADDRESS (if different from Controlling Office)
DAAG29-76-G-0189

15. SECURITY CLASS. (of this report)
Unclassified

15a. DECLASSIFICATION/DOWNGRADING SCHEDULE
NA

16. DISTRIBUTION STATEMENT (of this Report)

35 p.

Approved for public release; distribution unlimited.

17. DISTRIBUTION STATEMENT (of the abstract entered in Block 20, if different from Report)

NA

ARO 13807.1-PX

18. SUPPLEMENTARY NOTES

The findings in this report are not to be construed as an official Department of the Army position, unless so designated by other authorized documents.

19. KEY WORDS (Continue on reverse side if necessary and identify by block number)

Absorption, High Field, High Pressure

20. ABSTRACT (Continue on reverse side if necessary and identify by block number)

A high pressure optoacoustic cell has been calibrated over the pressure range from 5 to 35 atm using the pressure-induced absorption in N_2. Attempts to measure electric field-induced absorption in N_2 near 4.4μm using a carbon arc source have been unsuccessful because of insufficient spectral power density.

micrometers

DD FORM 1 JAN 73 1473 EDITION OF 1 NOV 65 IS OBSOLETE

Unclassified

SECURITY CLASSIFICATION OF THIS PAGE (When Data Entered)

AB

404668

1. Introduction

This document reports the results of an investigation of electric field-induced dipole absorption in molecular nitrogen. The study was motivated by the expectation that if the field-induced absorption cross-sections are reasonably large, a new type of high energy laser might be made available.

2. Discussion of Technical Work

The study of electric field-induced dipole absorption in molecular hydrogen has been described by various authors,[1-3] and observation of the effect in N_2 has been reported by Courtois, et al.,[4] but to the writer's knowledge no studies of N_2 have been reported. Integrated absorption coefficients for H_2, as reported by Crawford and MacDonald,[1] are of the order of $0.1\ cm^{-1}$ for field strengths in the range of 30 KV/cm to 75 KV/cm at a pressure of 89 atmospheres. The absorption in H_2 occurs in the region of 2.4μ.

The technique chosen for this experiment is that of optoacoustic spectroscopy, using an incoherent carbon arc as the exciting source. An advantage of this method is that the signal from the detector is proportional to the absorbed power, a significant factor in measurement of small total absorption. A special acoustically resonant high pressure cell was constructed for this experiment under a previous grant from the U.S. Army Research Office (Grant No. DAHC04 75 G 0198) and is described in the final report for that Grant. A

schematic drawing of the cell is shown as Fig. 1.

a. Optoacoustic Detector Calibration. While some preliminary calibration of the high pressure optoacoustic cell had previously been done using the 3.39μ methane absorption with a HeNe laser source, additional calibration was necessary prior to the measurement of field induced absorption. The additional calibration was done by using the cell to measure integrated pressure-induced absorption in N_2 with the carbon arc lamp as source.

The large area cylindrical microphone response exhibited a significant decrease with pressure over the range of 1 to 25 atm. A larger, less pressure-sensitive response was obtained by replacing the cylindrical microphone with an array of 3 small area electret microphones (Knowles Electronics, Inc., e.g., Model 1671). These microphones were installed with their diaphragms at holes in a cylindrical tube which replaced the perforated copper tube shown in Fig. 1. The outputs of these microphones were combined using an operational amplifier adder having appropriate phasing control on the three inputs. Representative results of measurements of integrated pressure-induced absorption in N_2, at 5, 15, and 25 atm, as a function of chopping frequency of the incident light, are shown in Fig. 2. These results show that there is no significant change in the acoustic resonance characteristics of the cell over this pressure range.

To obtain a calibration of the microphone and optoacoustic detector the measurements of integrated pressure-induced absorption in N_2 were compared with results reported by Shapiro and Gush.[5] Calculations were made on the assumption of uniform incident intensity over the N_2 pressure-induced absorption band which is centered at $\sim 4.41\mu$. The total incident power in this band was less than 1 mw and was unmeasurable with available instrumentation. The results of this calculated calibration, over the pressure range of 5 to 35 atm, are given in Fig. 3. These results indicate a decrease in microphone sensitivity of a factor of 5 over this pressure range.

b. The Carbon Arc Exciting Source. A filtered dc carbon arc has been used in all work during this grant period. Although the arc is a reasonable approximation of a 5500°K black body source, its use presented, what eventually turned out to be, insurmountable experimental difficulties. These difficulties can be described in three categories, namely: 1) intensity instabilities within the arc; 2) positional instabilities both of the arc itself and of the rods and; 3) inadequate useable narrow-band optical power in the spectral region of interest (near 4.4μ) . These problems are discussed separately below.

It was initially believed that both types of instability could be remedied by careful redesign of both the arc lamp power supply

and the mechanical construction of the rod feed mechanism. After considerable work on both of these features some improvement was obtained, but the remaining instabilities introduced so much noise onto the detector output that signal extraction proved impossible, even using phase-sensitive techniques.

The most serious obstacle to completion of the objective of this investigation was the inadequate useable narrow-band optical power in the spectral region near $4.4\mu m$. The spectral features to be detected are narrow lines (linewidth $\sim 1\ cm^{-1}$) superimposed on a broad band ($\sim 250\ cm^{-1}$) pressure-induced absorption. Therefore if the field-induced absorption is to even be observed the linewidth of the exciting source must be no wider than a few cm^{-1} . The useable optical power actually obtained in this bandwidth was of the order of a few microwatts, which was a factor of 10^3 less than was initially anticipated.

3. Summary of Principal Results

The following principal conclusions can be drawn from this investigation:

(a) A high pressure optoacoustic cell is a practical device for measurement of absorption spectra of gases at high pressure. Microphone response, while attenuated at pressures above atmospheric, is adequate. The response of the system described in this report is reduced by a factor of 5 as pressure is increased from 5 to 35 atm.

(b) A carbon arc lamp is an inadequate source for optoacoustic detection and measurement of electric field-induced absorption in N_2, principally because of inadequate spectral brightness in the 4.4μm region.

4. List of Publications

P. C. Claspy and Yoh-Han Pao, "Parameter Studies Relative to an Electric Field-Induced Dipole Moment Laser," Proceedings of U.S. Army Symposium on New Concepts in High Energy Lasers, Readstone Arsenal, Ala., Dec. 1976.

5. List of Participating Scientific Personnel

Professor P. C. Claspy, Principal Investigator

Professor Sheldon Gruber

Mr. Eugene Nodov

Mr. Chang Ha

Mr. Douglas Blakeley

Mr. K. P. Koo

Mr. Francis Merat

List of References

1. Crawford, M. F. and R. E. MacDonald, "Field-Induced Absorption in Hydrogen," Can. J. Phys. 36, 1022 (1958).

2. Boyd, W. J., P. J. Brannon, and N. M. Gailar, "Higher Electric Fields for Stark-Induced Infrared Spectra," Appl. Phys. Letters 16, 135 (1970).

3. Buijs, H. L. and H. P. Gush, "Static-Field Induced Spectrum of Hydrogen," Can. J. Phys. 49, 2366 (1971).

4. Courtois, D., C. Thiebeaux, and P. Jouve, "Spectre d'absorption infrarouge de la molécule d'azote indiut par un Champ électrique," C. R. Acad. Sc. Paris, Series B, 274, 744 (1972).

5. Shapiro, M. M. and H. P. Gush, "The Collision-Induced Fundamental and First Overtone Bands of Oxygen and Nitrogen," Can. J. Phys. 44, 949 (1966).

List of Figures

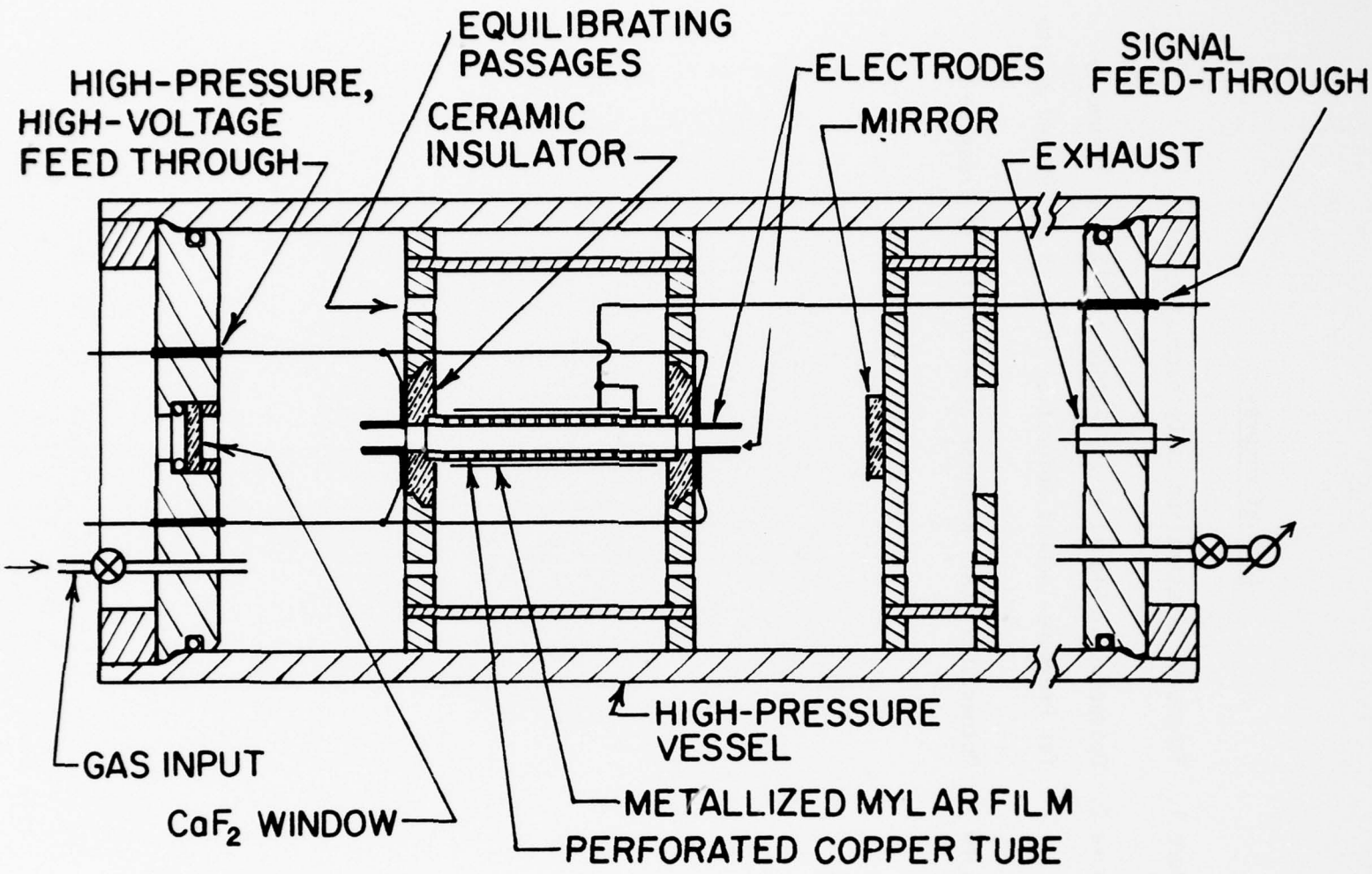
EQUILIBRATING PASSAGES
HIGH-PRESSURE, HIGH-VOLTAGE FEED THROUGH
CERAMIC INSULATOR
ELECTRODES
MIRROR
SIGNAL FEED-THROUGH
EXHAUST
HIGH-PRESSURE VESSEL
GAS INPUT
CaF_2 WINDOW
METALLIZED MYLAR FILM
PERFORATED COPPER TUBE

Figure 1

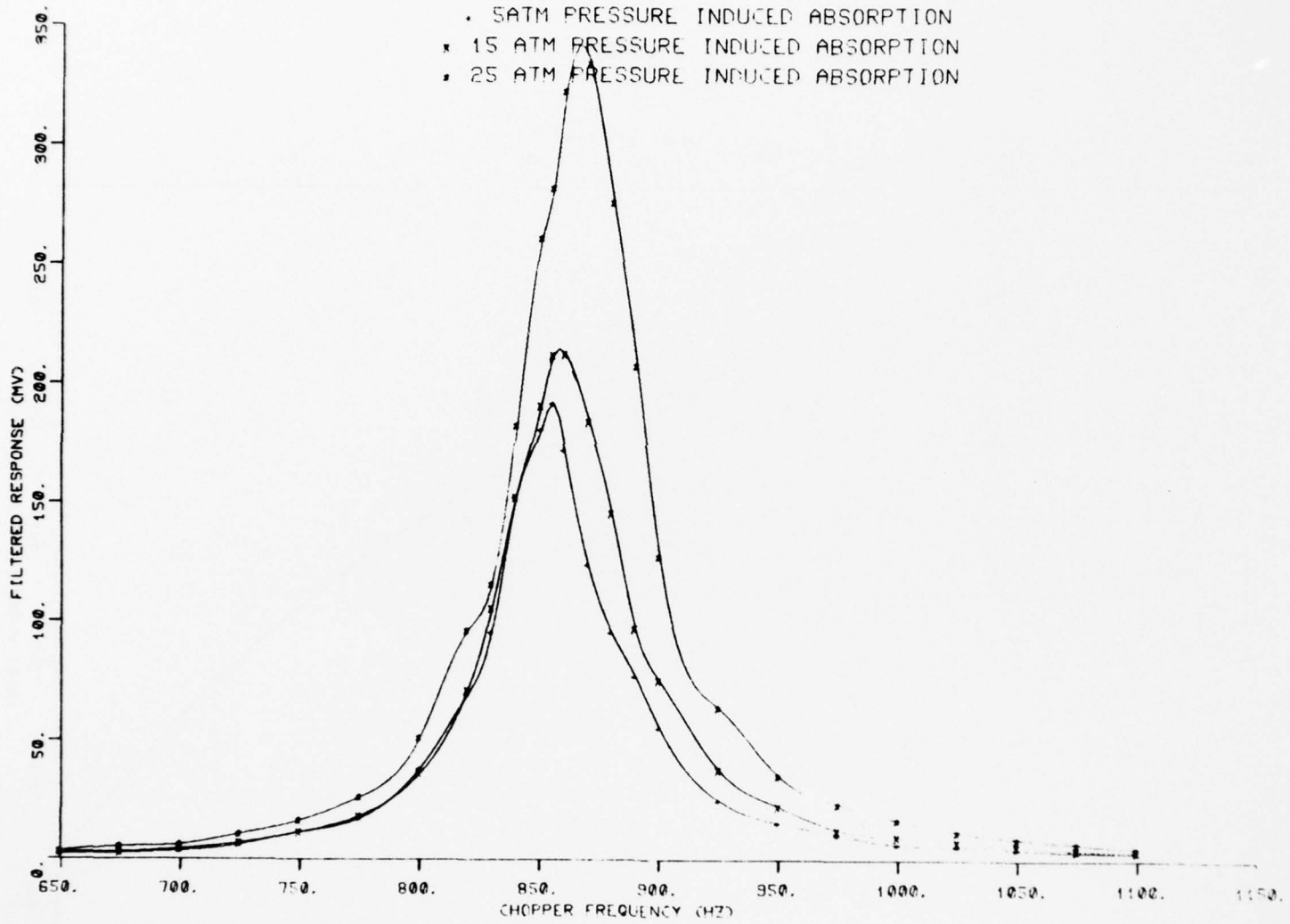
. 5ATM PRESSURE INDUCED ABSORPTION
x 15 ATM PRESSURE INDUCED ABSORPTION
* 25 ATM PRESSURE INDUCED ABSORPTION
FILTERED RESPONSE (MV)
0.
50.
100.
150.
200.
250.
300.
350.
650.
700.
750.
800.
850.
900.
950.
1000.
1050.
1100.
1150.
CHOPPER FREQUENCY (HZ)

Figure 2

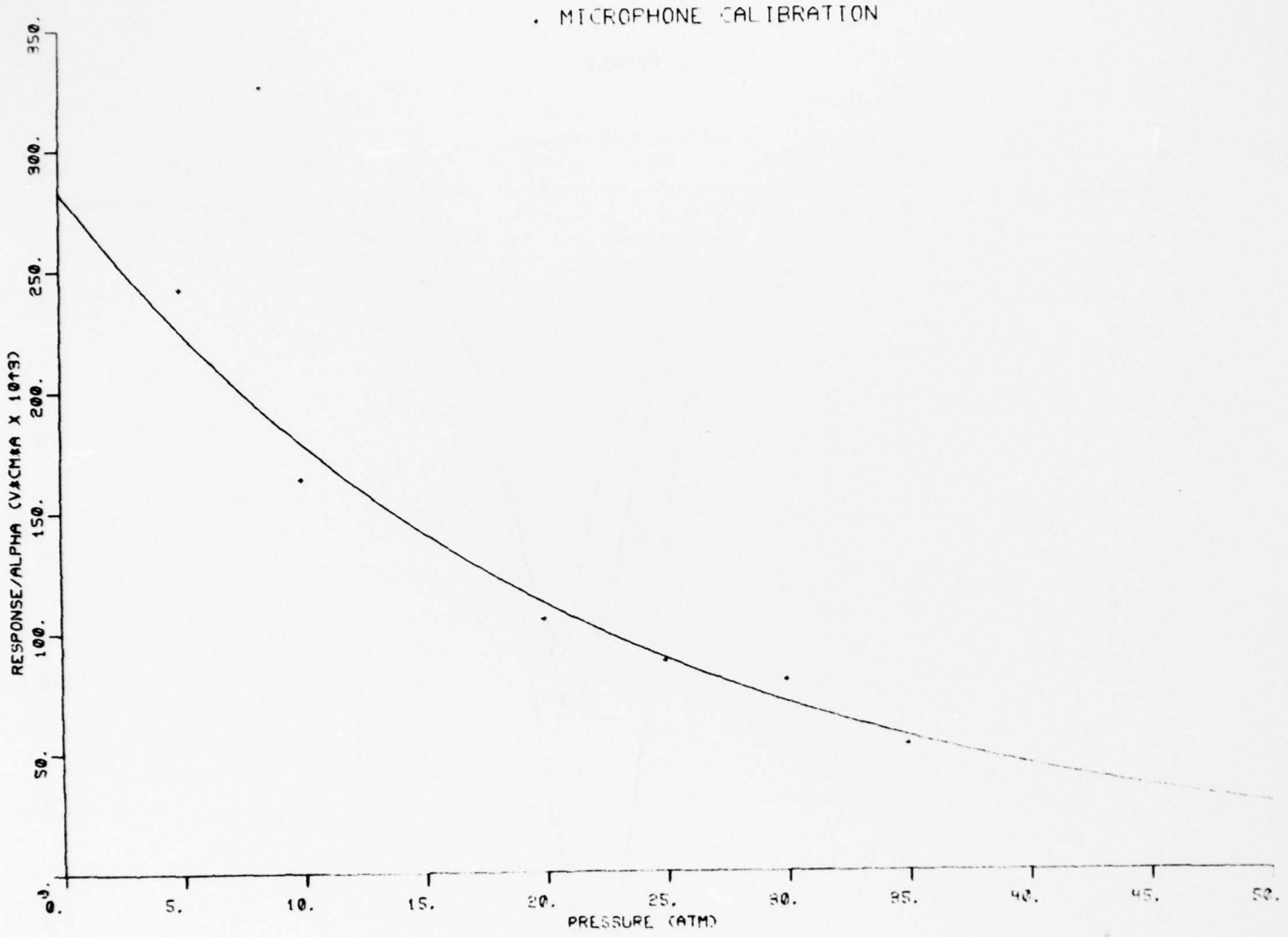
MICROPHONE CALIBRATION
RESPONSE/ALPHA (VACM&A X 1013)
0.
50.
100.
150.
200.
250.
300.
350.
0.
5.
10.
15.
20.
25.
30.
35.
40.
45.
50.
PRESSURE (ATM)

Figure 3

Appendix 1

PARAMETER STUDIES RELATIVE TO AN ELECTRIC FIELD-INDUCED DIPOLE MOMENT LASER: A PROGRESS REPORT

P. C. Claspy and Yoh-Han Pao
Department of Electrical Engineering and Applied Physics
Case Western Reserve University
Cleveland, Ohio 44106

Presented at

U.S. Army Symposium on New Concepts in High Energy Lasers,
Redstone Arsenal, Alabama, 30 November 1976.

PRAMETER STUDIES RELATIVE TO AN ELECTRIC FIELD-INDUCED DIPOLE MOMENT LASER: A PROGRESS REPORT

P. C. Claspy and Yoh-Han Pao
Department of Electrical Engineering and Applied Physics
Case Western Reserve University
Cleveland, Ohio 44106

Abstract

A theoretical discussion of electric field-induced absorption in homonuclear diatomic molecules and preliminary results of an experiment to measure this effect in N_2 using a high pressure optoacoustic detector are presented. The theoretical results show that this effect can potentially be used as a new and attractive high energy laser. The preliminary experimental results, obtained using a carbon arc as the source, show that while it is possible to observe pressure-induced absorption at pressures of the order of 30 atm, measurement of electric field-induced absorption depends on the availability of a more stable, brighter source than the carbon arc.

PARAMETER STUDIES RELATIVE TO AN ELECTRIC FIELD-INDUCED DIPOLE MOMENT LASER: A PROGRESS REPORT

Ordinarily, homonuclear diatomic molecules can neither absorb nor emit infrared radiation. This is because vibrations in such molecules do not give rise to oscillating dipole moments capable of interacting resonantly with the radiation field. Consequently, in such systems, excited vibrational states do not decay because of spontaneous emission. Similarly, absence of an electric dipole moment results in a small cross-section for de-excitation of excited vibrational states by intermolecular collisions. Both these reasons ensure that in homonuclear diatomic gases vibrationally excited states have long lifetimes, especially at moderate pressure.

For such molecules, resonant interaction with infrared radiation can be made allowed through the mechanism of intermolecular collisions or through the action of an externally applied electric field.[1] The latter mechanism is of particular interest since external electric fields can be applied or removed readily in controlled manner.

The electric field may be a static field or a dynamic field; it induces a dipole moment in the molecule, the magnitude of which is determined by the square of the product of the polarizability and the field strength. Vibration and rotation of the molecule modulate this electric dipole and resonant interaction with radiation field becomes allowed.

For homonuclear diatomic gases, this combination of long-lived excited vibrational states and field induced emission presents the possibility of a new laser system in which the former effect would permit the storage of considerable energy in excited vibrational states and the second effect would permit laser action when desired on demand.

Basov[2] has suggested for example, that hydrogen might be pumped with an electron beam and subsequently triggered to emit high energy and high peak power pulses by irradiating it with CO_2 laser radiation pulses, using the optical electric field to induce the dipole moment.

However, other less difficult and perhaps more interesting systems can also be visualized, one of which might be a thermally pumped gas dynamic laser in which the hot nitrogen gas is expanded to a low rotational temperature. The $\Delta J = +2$ transition allowed in the field induced effect would allow laser action to occur over partially inverted vibrational-rotational states.

Partial inversion is more readily attained for $\Delta J = +2$ (emission) transitions than for $\Delta J = +1$ transitions. In view of this, we investigated in further detail the conditions for which partial inversion might be attained. This interest in the possibility of partial inversion does not mean that gas dynamic laser schemes are of primary interest but rather that if partial inversion is easily attained, then excitation requirements might not be very demanding regardless of the excitation scheme to be used.

If we let N_2 and N_1 represent respectively the populations of the upper and lower vibrational-rotational levels of the laser transition, then the populations are as shown below.

$$N_2 \sim e^{-E_v(2)/kT_v}[2J + 1]\, e^{-BJ(J+1)/kT_r} \tag{1}$$

$$N_1 \sim e^{-E_v(1)/kT_v}[2(J+2) + 1]\, e^{-B(J+2)(J+3)/kT_r} \tag{2}$$

where T_v and T_r are the vibrational and rotational temperatures and all the other symbols have their usual thermodynamics and spectroscopic meanings.

In order that partial inversion be attained, it is necessary that $N_2/N_1 > 1$ or equivalently,

$$\left(\frac{2J+5}{2J+1}\right) \exp[\Delta E_v/kT_v - B(4J+6)/kT_r] < 1 \quad \text{(for } J \to J+2 \text{ transition)} \tag{3}$$

This condition is more easily satisfied than the similar one for $\Delta J = +1$, which applies for molecules having a permanent dipole moment. For large and small J, the partial inversion condition reduces to those shown below.

For large J, Eq. (3) reduces to

$$T_v > T_r\, \Delta E_v/4BJ$$

while for $J \to 0$, $T_v > T_r\, \Delta E_v/(6B - 1.66\, kT_r)$

We will consider two molecules in some detail namely hydrogen and nitrogen. Table 1 shows calculated transition energies for hydrogen for several transitions in which $\Delta v = -1$, $\Delta J = +2$. The transitions enclosed by boxes occur at wavelengths for which atmospheric absorption is expected to be small. Considering the possibilities for partial inversion to obtain laser action on any of these, we note that the rotational constant, B , for hydrogen is 60 cm^{-1} , which is rather large. This means that at reasonable rotational temperatures, T_r , J is most likely to be small, say 0 or 1 . If we select $T_v \sim 1200°K$ to populate the $v = 4$ and $v = 5$ levels significantly, then, using the condition for small J , $T_r \sim 150°K$. These temperatures are reasonably attainable, but permit only a few of the transitions of primary interest to occur.

For nitrogen, conditions are actually more favorable, as illustrated in Table 2. In this table, all transitions to the lower right of the dividing line are of interest in so far as atmospheric transmission is concerned. The molecular constant B is small, being approximately 2 cm^{-1}, and therefore large J values (> 20) may be expected even at moderate rotation temperatures. For J greater than 30, the condition for partial inversion, is that $T_v > 10\ T_r$. Again, just as it was in the case of hydrogen, it means that T_r would have to be less than 150°K.

On the basis of these calculations we have decided to carry out an investigation of the induced absorption in nitrogen. Measurements of field-induced absorption in hydrogen have been reported by Crawford and

MacDonald[3] and some of their results are shown in Fig. 1. In this figure, the dashed curve indicates pressure-induced absorption and the solid curve the electric field-induced absorption. (Density units--1 Amagat = density at 1 Atm pressure.) Note that the lines are extremely narrow, about 0.5 cm^{-1}, even at 84 atm pressure.

Figure 2 is a plot of integrated absorption coefficient vs field strength at 84 Amagat for the Q(1) component, as reported by the same authors.

These results are shown because they were used for measurement feasibility calculations for N_2. Since the polarizabilities of N_2 and H_2 are nearly equal, the results for H_2 were used in our calculations.

Before going on to a description of the apparatus to be used to study induced absorption, it is useful to take a brief look at a second induced absorption effect. Since it is possible to polarize a nonpolar molecule with an external dipolar electric field, it should also be possible to polarize it with the quadrupolar field of a second molecule. This effect has, in fact, been observed and is known as pressure-induced, or density-induced absorption. The results of the measurement of this effect in N_2 at 18.4 Amagat, as reported by Shapiro and Gush,[4] are shown in Fig. 3. The broadening seen here, which is much greater than that seen in the external field-induced effect at the same pressure occurs because the induced dipole moment is only large during the time of close collision. The result of this is to provide an apparent increase in the

effective pressure. Figure 4 is a plot of integrated pressure-induced absorption coefficient in N_2 as a function of density (pressure), as reported by Shapiro, et al. If we assume that the external-field-induced absorption in N_2 is the same as that reported by Crawford and MacDonald for hydrogen, the integrated external field-induced absorption coefficient at 40 Atm and 24 kV/cm is about 100 times the pressure-induced absorption. Before accurate predictions of field-induced (or pressure-induced) laser operation can be made, measurements of the field-induced effect in N_2 are necessary.

To measure both field-induced absorption and pressure-induced absorption we are using a high pressure optoacoustic cell.

Before describing the cell a brief word should be said about the optoacoustic effect.[5] When light of an appropriate frequency is incident on an absorbing gas, some of the gas molecules absorb and become vibrationally excited. Then, as a result of collisions with other molecules, that energy is converted into kinetic energy, resulting in a temperature increase. If the gas is confined and the light is chopped, an acoustic wave is generated in the cell. The acoustic wave is then detected by a sensitive microphone which is also inside the cell. The advantage of such a system is that the signal is proportional to the absorbed power and one is not faced with the task of measuring a small difference between two nearly equal large numbers as in the conventional absorption coefficient measureing experiment.

Our cell which is shown schematically in Fig. 5, is designed as an acoustic resonator, with a resonant frequency of ∿ 1150 Hz. The microphone is a cylindrical capacitive device consisting of a brass inner sleeve with holes, wrapped with aluminized mylar. A 90 v battery is placed across the capacitor and the signal is the current flow resulting from pressure modulation of the capacitance. The cell housing is a specially modified 6½ in. I.D. by 22 in. long hydraulic accumulator[6] which has been tested to 4500 psi. The optical window is 0.75 in. dia by 0.20 in. thick CaF_2 having a calculated maximum working pressure of 2400 psi. The electrical connections, both signal and high voltage, are through CONAX[7] high pressure feed-throughs. The completed cell has been hydrostatically tested to 1300 psi and has been operated at gas pressures to 600 psi (40 Atm).

The microphone is supported in the center of the cell by two lava[8] insulated aluminum discs. 5 cm long parallel plate electrodes have been placed at each end and are supported by the lava insulators. Electrode separation is adjustable and a maximum electric field of ∿ 60 kV/cm, with an electrode separation of 3 mm is available. The present electrode design represents a compromise between an adequate width-to-separation aspect ratio to provide a uniform field on the one hand and a minimum size to prevent interference with a radial acoustic vibrational mode on the other hand. Because of uncertainties about the effectiveness of the current electrode configuration in adequately meeting either requirement, the electrode system is being redesigned. The new design will consist of

a small number of small diameter wires arrayed along a circular cylindrical surface, with appropriate voltage variation from wire to wire. This configuration is expected to more adequately meet both criteria.

To insure microphone operation at elevated pressures the cell has been tested at several pressures between 1 atm and 40 atm, using methane diluted in N_2 as the absorber and a HeNe laser operating on the 3.39μ transition as the source. In this experiment an unknown but small quantity of methane was mixed with pure N_2, at 1 Atm, in the cell and the optoacoustic signal, resulting from absorption of 3.39μ radiation, was measured as a function of chopping frequency. The results of this measurement are shown in Fig. 6. This shows a resonant frequency of $\sim$ 1150 Hz and an acoustic Q of $\sim$ 11. The cell was then pressurized by adding pure N_2 and similar data were taken at 10 Atm increments. Figure 7 shows a typical result, taken at 30 Atm absolute, or 450 psi. Here we see that the resonant frequency has shifted downward slightly and the acoustic Q has dropped to perhaps 8, indicating that some microphone damping has occurred, as expected. The fact that the peak signals at the two pressures do not agree would appear, on the basis of later experiments to be the result of inadequate mixing time at 1 Atm. The cell has been calibrated by performing similar measurements with a calibrated gas mixture of 507 ppm methane in N_2. From data reported by Kreuzer,[9] the absorption coefficient of 1 atm of this mixture at 3.39μ is $4\times10^{-3}cm^{-1}$. With $\sim$ 5 mw of 3.39μ radiation a signal of 8 μV, with a signal-to-noise of $\sim$ 100, was obtained, indicating an extrapolated

sensitivity of $2\times10^{-4}cm^{-1}$ per milliwatt with a signal-to-noise of 1. This is a somewhat lower sensitivity than has been obtained with other similar cells in our laboratory,[10,11] indicating that perhaps electrode interference with acoustic vibration is occurring.

We have used a filtered DC carbon arc lamp as a source. While the lamp is a reasonable approximation of a 5500°K black body source, the instabilities in position of the arc and hot rods have been the greatest source of difficulty in these experiments. In preliminary measurements we have used a Ge slab as a short wavelength filter and the CaF_2 window as a long wavelength filter. We have also constructed a prism monochromator, as shown in Fig. 8 to provide somewhat better resolution. All of the experiments to date using the arc lamp have been performed with Ge - CaF_2 filter system.

We have observed the pressure-induced absorption in N_2 using the arc lamp, at pressures between 1 atm and 30 atm. The measurement has been rather qualitative, however, since the arc lamp instabilities have increased the noise level to the point that signal-to-noise ratios at 10 μV signal levels are only about 2-3, even with a 10 sec integration time. Attempts have been made to measure the electric field-induced absorption in N_2 at electrode voltage differences up to 12 kV, giving a nominal field strength of 24 kV/cm. The results here have been inconclusive both because of the high noise level of the arc lamp and because of field uniformity uncertainties discussed earlier. In addition, when

using a broadband source such as ours, the calculated power absorbed by the pressure induced absorption is $\sim$ 5 times that absorbed as a result of 24 kV/cm field-induced absorption. Several modifications of the experiment are being investigated in order to remedy this situation. First, the improved electrode design should increase cell sensitivity and field uniformity. Second, larger electric fields are possible. Third, modulation of the electric field is being considered as an alternative to light chopping. In this mode, if detection is synchronous with the field modulation the pressure induced effect will not appear in the signal. Based on our experience in other optoacoustic experiments, however, it is apparent that the availability of an improved tunable, narrowband source, such as a diode laser, is important to the continuation of this investigation.

In conclusion, an electric field-induced dipole moment system appears to offer interesting possibilities for a high energy laser. While no particular effort has been made to investigate excitation and population inversion schemes, a thermally excited, expansion cooled gasdynamic system may be possible. Another possible excitation scheme could use the atmospheric reaction between atomic Nitrogen and NO_2 , which produces vibrationally excited N_2 .

We wish to acknowledge the significant contribution of our colleague, Professor Sheldon Gruber, to the work reported here. This work has been supported by a grant from the U.S. Army Research Office, Durham, N. C.

References

1. Condon, E. V., "Production of Infrared Spectra with Electric Fields", Phys. Rev. 41, 759 (1932).

2. Basov, N. G., A. N. Oraevskii, and A. F. Suchkov, "Possibility of Generating Ultrashort Laser Pulses on Combination Vibrational-Rotational Transitions of Molecular Hydrogen", JETP Letters 16, 211 (1972).

3. Crawford, M. F. and R. E. MacDonald, "Field-Induced Absorption in Hydrogen", Can. J. Phys. 36, 1022 (1958).

4. Shapiro, M. M. and H. P. Gush, "The Collision-Induced Fundamental and First Overtone Bands of Oxygen and Hydrogen", Can. J. Phys. 44, 949 (1966).

5. For additional discussion of the optoacoustic effect see, e.g., Optoacoustic Spectroscopy, ed. by Yoh-Han Pao, Academic Press (in press).

6. Supplied by Superior Hydraulics Div., Superior Pipe Specialties Co., Cicero, Ill.

7. Supplied by CONAX Corp., Buffalo, N. Y.

8. Supplied by Technical Ceramic Products Div., 3M Co., Chattanooga, Tenn.

9. Kreuzer, L. B., "Ultralow Gas Concentration Infrared Absorption Spectroscopy", J. Appl. Phys. 42, 2934 (1971).

10. Claspy, P. C., Chang Ha, and Yoh-Han Pao, "Application of Pulsed Dye Laser to Optoacoustic Detection of NO_2", J. Opt. Soc. 66, 1072 (1976).

11. Claspy, P. C. Yoh-Han Pao, S. Kwong, and E. Nodov, "Laser Optoacoustic Detection of Explosive Vapors", Applied Optics 15, 1506 (1976).

Fig. 1 Electric field-induced absorption in hydrogen at a density of 84 Amagat.[3]

Fig. 2 Integrated electric field-induced absorption coefficient for the Q_1 component of hydrogen as a function of applied electric field.[3]

Fig. 3 Fundamental pressure-induced absorption band in nitrogen for a 40 m path at 18.4 Amagat.[4]

Fig. 4 Integrated pressure-induced absorption coefficient of the nitrogen fundamental band as a function of nitrogen density.[4]

Fig. 5 Schematic illustration of optoacoustic cell.

Fig. 6 Optoacoustic signal as a function of chopping frequency for 1 atm methane - N_2 mix and 3.39μ radiation.

Fig. 7 Optoacoustic signal as a function of chopping frequency for 30 atm methane - N_2 mix and 3.39μ radiation.

Fig. 8 Schematic illustration of prism monochromator.

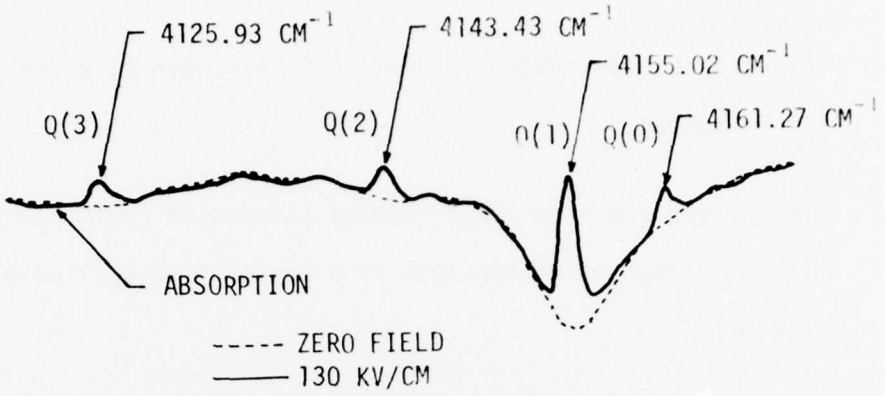

Figure 1

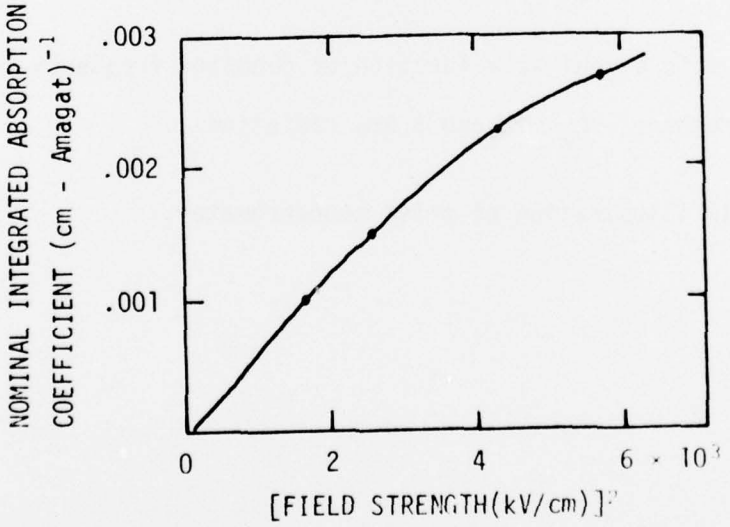

Figure 2

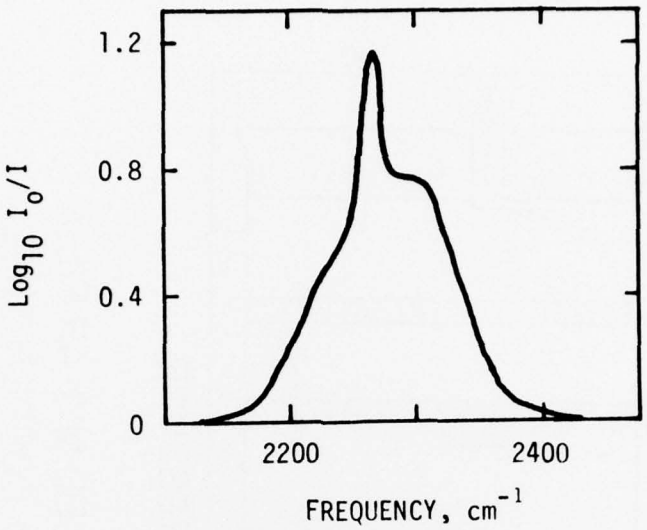

Figure 3

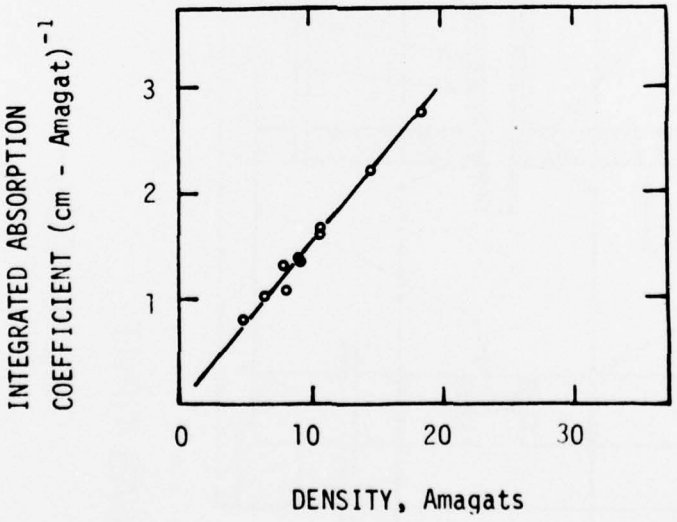

Figure 4

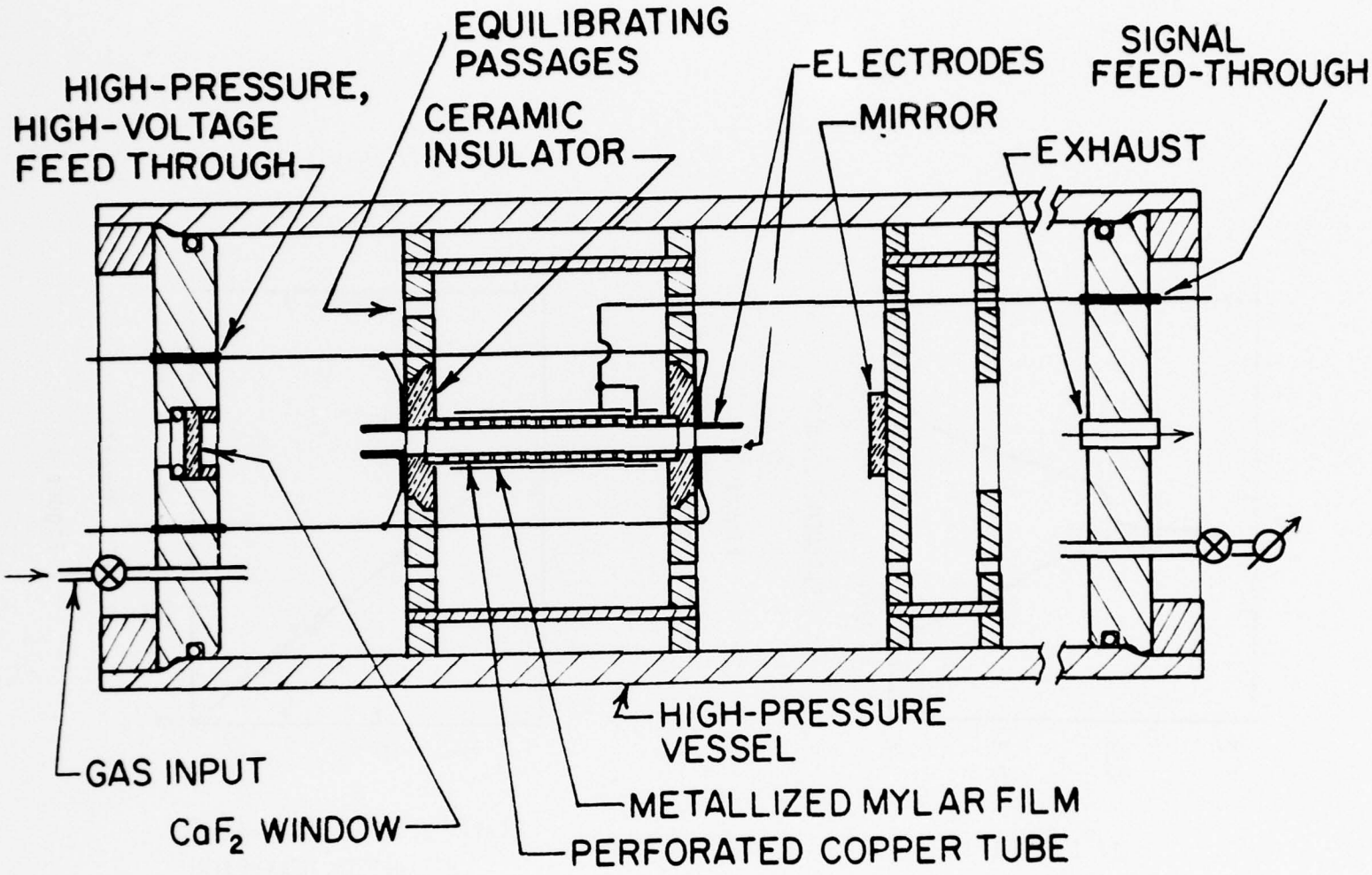
EQUILIBRATING PASSAGES
ELECTRODES
SIGNAL FEED-THROUGH
HIGH-PRESSURE, HIGH-VOLTAGE FEED THROUGH
CERAMIC INSULATOR
MIRROR
EXHAUST
HIGH-PRESSURE VESSEL
GAS INPUT
CaF_2 WINDOW
METALLIZED MYLAR FILM
PERFORATED COPPER TUBE

Figure 5

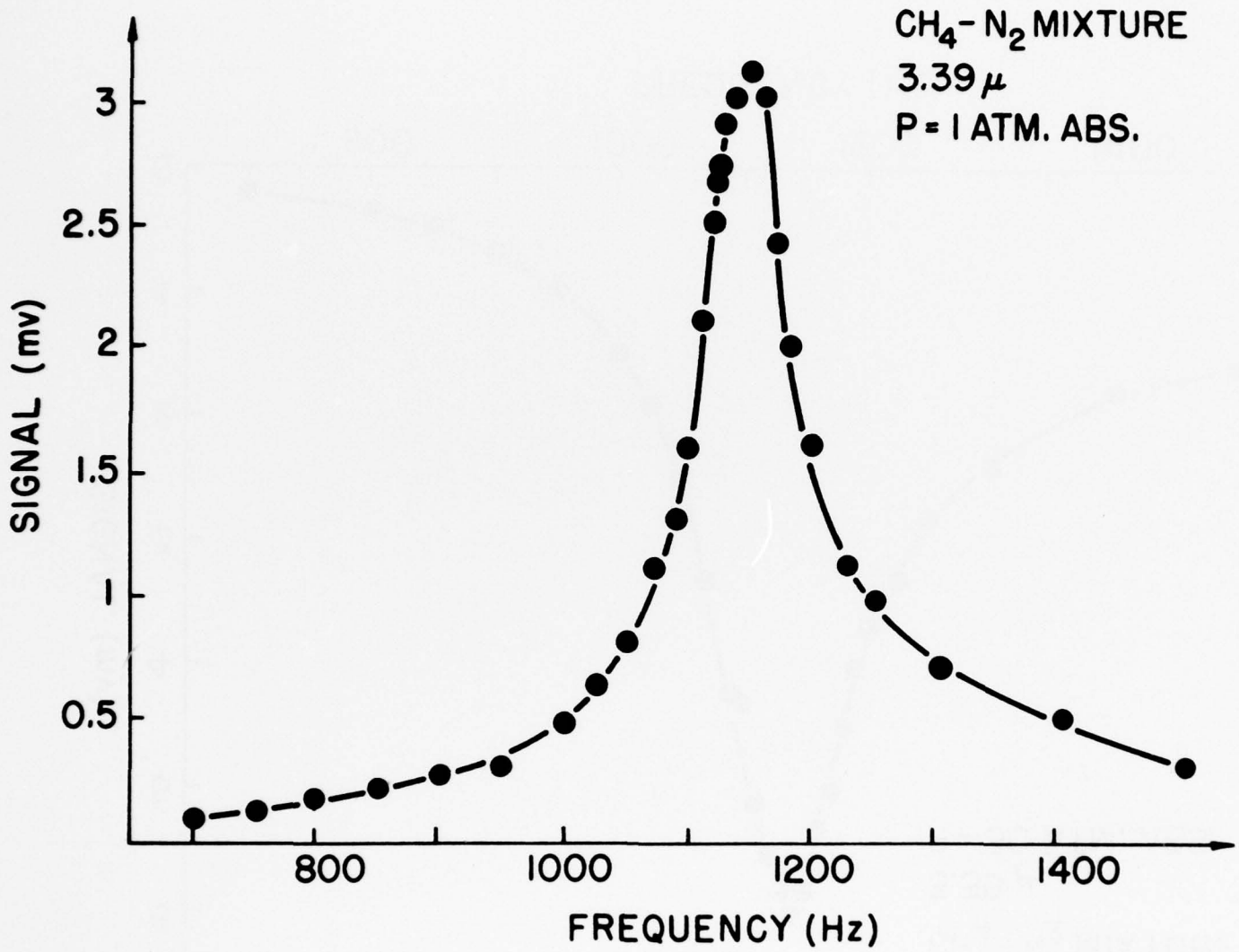
$CH_4 - N_2$ MIXTURE
3.39 μ
P = 1 ATM. ABS.
SIGNAL (mv)
3
2.5
2
1.5
1
0.5
800
1000
1200
1400
FREQUENCY (Hz)

Figure 6

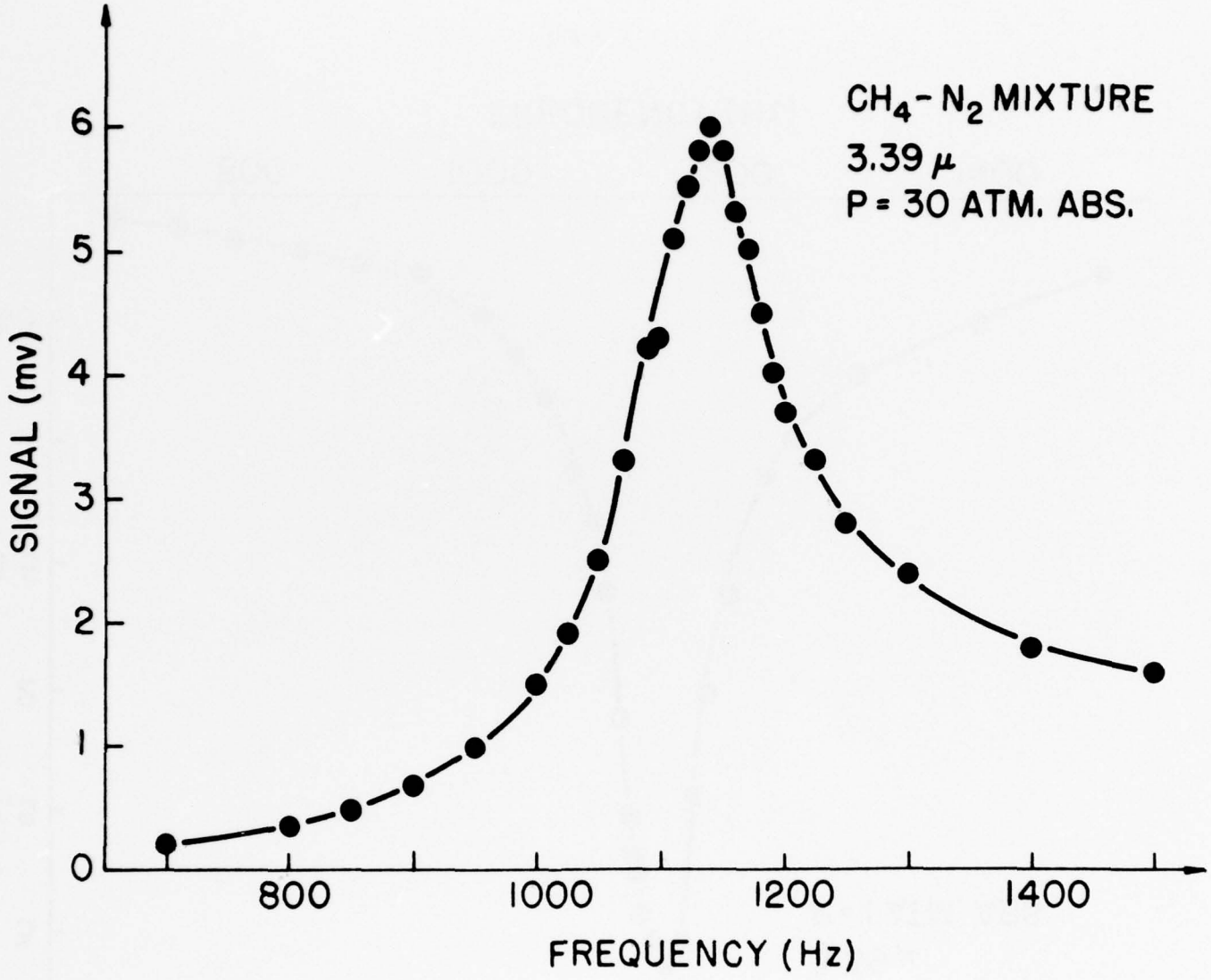
$CH_4 - N_2$ MIXTURE
3.39 μ
P = 30 ATM. ABS.
SIGNAL (mv)
0
1
2
3
4
5
6
800
1000
1200
1400
FREQUENCY (Hz)

Figure 7

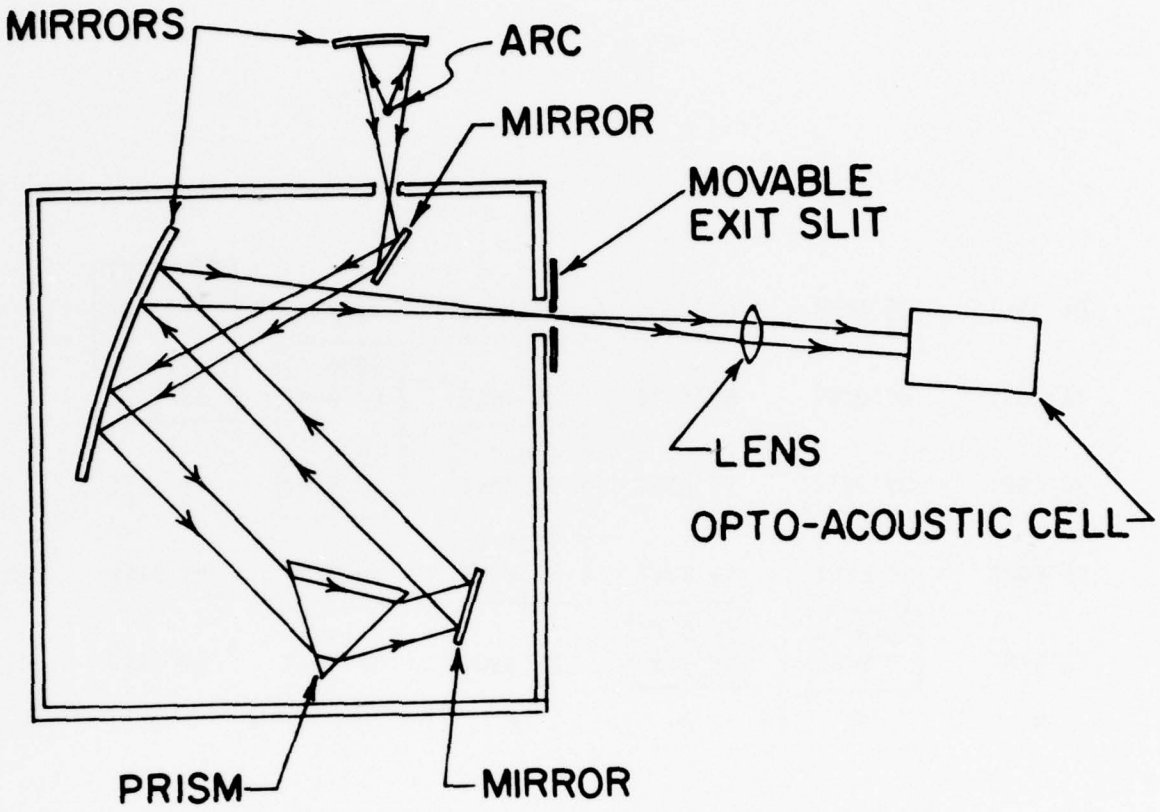
MIRRORS
ARC
MIRROR
MOVABLE
EXIT SLIT
LENS
OPTO-ACOUSTIC CELL
PRISM
MIRROR

Figure 8

TABLE 1

Variation of Hydrogen Transition Energies (cm^{-1}) and Wavelengths (microns) with Upper State Vibration and Rotation Quantum Numbers. (v, J → v-1, J + 2)

v = /J =	0	1	2	3	4	5	6
1	3795.42	3551.22	3308.02	3064.82	2821.62 (3.878)	2578.4 (3.878)	2335.22
2	3559.44	3315.24	3072.04	2828.84 (3.535)	2585.64	2342.44	2099.24
3		3079.26	2836.04 (3.526)	2592.86 (3.857)	2349.66	2106.46	1863.26
4		2843.28 (3.517μ)	2600.08 (3.846)	2356.88	2113.68	1870.48	1627.28
5		2607.30 (3.84μ)	2364.10	2120.90	1877.70	1634.50	1391.30

TABLE 2

Variation of Nitrogen Transition Energies (cm^{-1}) and Wavelengths (microns)

With Upper State Vibration and Rotation Quantum Numbers (v, J → v-1, J + 2)

v/ J =	0	1	2	3	4	5	6	10	20
1	2318.64	2310.60	2302.56	2294.52	2286.48	2278.44	2270.40	2238.24	2157.84 (4.634μ)
2	2289.72	2281.68	2273.64	2265.60	2257.56	2249.52	2241.48		
3	2260.81	2252.77	2244.73	2236.69	2228.65	2220.61	2212.57		
4	2231.90 (4.482μ)	2223.86 (4.498)	2215.82 (4.514μ)	2207.78	2199.74	2191.70	2183.66		
5	2202.99 (4.539μ)	2194.95	2186.91	2178.87	2170.83	2162.79	2154.75 (4.641μ)	2122.95 (4.710μ)	2022.91 (4.943μ)